Neoplasia 57 (2024) 101047

Contents lists available at ScienceDirect

Neoplasia

journal homepage: www.elsevier.com/locate/neo

Original Research

PLXNA1 confers enzalutamide resistance in prostate cancer via AKT signaling pathway

Jing Hu [a,b,1], Jing Zhang [c,1], Bo Han [d,1], Ying Qu [e], Qian Zhang [f], Zeyuan Yu [g], Lin Zhang [h], Jingying Han [g], Hui Liu [a], Lin Gao [g], Tingting Feng [g], Baokai Dou [c], Weiwen Chen [i], Feifei Sun [a,*]

[a] Department of Pathology, Qilu Hospital, Shandong University, Jinan 250012, China
[b] Michigan Center for Translational Pathology, University of Michigan, Ann Arbor, MI, USA
[c] Department of Pharmacy, Shandong Provincial Hospital Affiliated to Shandong First Medical University, Jinan, Shandong, 250021, China
[d] Department of Pathology, Peking University People's Hospital, Beijing, China
[e] Department of Pharmacy, The Second Hospital, Cheeloo College of Medicine, Shandong University, Jinan, Shandong 250012, China
[f] Department of Pathology, Binzhou Medical University Hospital, Binzhou 256603, China
[g] The Key Laboratory of Experimental Teratology, Ministry of Education and Department of Pathology, School of Basic Medical Sciences, Shandong University, Jinan, Shandong, 250012, China
[h] Yinzhou District Center for Disease Control and Prevention, Ningbo, China
[i] Department of Biochemistry and Molecular Biology, School of Basic Medical Sciences, Jinan 250012, China

ARTICLE INFO

Keywords:
PLXNA1
Prostate cancer
Androgen receptor antagonists
Drug resistance
AKT

ABSTRACT

Although targeting the androgen signaling pathway by androgen receptor (AR) inhibitors, including enzalutamide, has shown therapeutic effectiveness, inevitable emergence of acquired resistance remains a critical challenge in the treatment of advanced prostate cancer (PCa). Recognizing targetable genomic aberrations that trigger endocrine treatment failure holds great promise for advancing therapeutic interventions. Here, we characterized PLXNA1, amplified in a subset of PCa patients, as a contributor to enzalutamide resistance (ENZR). Elevated PLXNA1 expression facilitated PCa proliferation under enzalutamide treatment due to AKT signaling activation. Mechanistically, PLXNA1 recruited NRP1 forming a PLXNA1-NRP1 complex, which in turn potentiated the phosphorylation of the AKT. Either inhibiting PLXNA1-NRP1 complex with an NRP1 inhibitor, EG01377, or targeting PLXNA1-mediated ENZR with AKT inhibitors, abolished the pro-resistance phenotype of PLXNA1. Taken together, combination of AKT inhibitor and AR inhibitors presents a promising therapeutic strategy for PCa, especially in advanced PCa patients exhibiting PLXNA1 overexpression.

Introduction

Prostate cancer (PCa) stands as the second most common malignancy affecting males worldwide [1]. Androgen deprivation therapy (ADT) has been successful in treating advanced PCa, yet it is not curative. However, most PCa patients develop castration-resistant prostate cancer (CRPC) within a few years after diagnosis. [2]. One of the key drivers of CRPC is the persistent androgen receptor (AR) signaling, including elevation of AR expression (e.g., *AR* amplification/mutation; increased protein stabilization), or activation of AR signaling through crosstalk pathways (e.g., AKT; glucocorticoid receptor pathway) [3]. Numerous androgen receptor signaling inhibitors have been developed to treat this AR addicted CRPC. However, these treatments, including enzalutamide, an intense AR inhibitor, initially display efficacy by prolonged progression-free survival, but ultimately leads to acquired drug resistance [4,5]. The intrinsic or acquired resistance to enzalutamide poses a significant challenge to the effective management of PCa. Therefore, it is crucial to understand the mechanism of enzalutamide resistance (ENZR) in order to develop new therapeutic strategy for PCa.

The discovery of multiple escape pathways driving ENZR has sparked renewed interest in investigating the role and interplay among non-AR signaling pathways. Exploration of mechanisms circumventing AR signaling, particularly AKT signaling pathway, has provided insights into the clinical implications of AKT inhibitors in PCa. Alterations in components of the AKT signaling pathway, including mutations, changes in expression levels, and variations in copy numbers, were

* Corresponding author at: Department of Pathology, Qilu Hospital, Shandong University, Jinan 250012, China.
E-mail address: sunfeifei1781@163.com (F. Sun).
[1] These authors contributed equally to this work.

https://doi.org/10.1016/j.neo.2024.101047
Received 13 July 2024; Received in revised form 28 August 2024; Accepted 28 August 2024

detected in primary tumors at rates between 34 % and 43 %. Whereas in metastatic tumors, these alterations were observed at rates ranging from 74 % to 100 % [6]. Emerging evidence suggests a crucial role for the AKT signaling pathway, enabling PCa systems to sustain proliferation within low-androgen environments [7]. Co-targeting the AR and AKT signaling pathways has shown promise as a therapeutic approach [8,9]. However, further investigation is needed to identify predictive biomarkers for this combination.

Plexin-A1 (PLXNA1) is a transmembrane receptor protein that belongs to the plexin family, which acts as the semaphorin receptor in the axon guidance pathway. Evidence reveals that axon guidance pathway extends beyond their role in development of central nervous system and potentially participates in carcinogenesis and tumor progression.

Recent studies have shown increased expression of PLXNA1 in various cancer types, such as breast cancer, lung cancer, and PCa, suggesting its potential as a broad biomarker for malignancies [10-13]. This overexpression has been closely tied to tumor progression, metastasis, and a poor prognosis [14-16]. The absence of PLXNA1 suppresses proliferation and invasion of glioblastoma stem cells [17]. Intriguingly, in the context of PCa, the *PLXNA1* copy number gain/amplification serves as an important event in Chinese population [9,18]. Axon guidance pathway rewires to an activate state upon ADT failure [19].

PLXNA1 overexpression ushers in a resistance to enzalutamide effects, whereas silencing PLXNA1 re-sensitize enzalutamide-resistant cells. The resistance induced by PLXNA1 was orchestrated through AKT pathway. Our study highlights translational promise of combining AKT inhibitors with enzalutamide in advanced PCa patients exhibiting *PLXNA1* copy number gain or amplification at the DNA level.

Materials and methods

PCa tissue and immunohistochemistry (IHC)

Our study included 171 patients diagnosed with PCa at Qilu Hospital between 2010 and 2015. Criteria for participant inclusion and exclusion are detailed in the **Supplementary Table 1**. Among the participants, there were142 locally primary PCa patients and 29 CRPC patients. Of these 142 primary PCa patients, 89 patients (62.6 %) received post-prostatectomy hormonal therapy, with 14 subsequently developed CRPC. Additional detailed information was available in **Supplementary Table 2**.

IHC was performed following established protocols as described previously [20]. Primary antibodies against PLXNA1, p-AKT and Ki67 were employed in this investigation. The IHC slides were blindly evaluated by two pathologists (H.L. and J.H.) to validate the expression of PLXNA1 and p-AKT, as previously described [20].

Cell culture

Human PCa cell lines LNCaP (CVCL_0395), DU145 (CVCL_0105), C4-2B (CVCL_4784), 22Rv1 (CVCL_1045), and PC3 (CVCL_0035) and HEK293T (CVCL_0063) were obtained from the ATCC and cultured following ATCC's instructions. All cell lines were validated to be devoid of mycoplasma contamination. Additionally, the cumulative duration of cell culture, from thawing to utilization in this study, did not exceed 15 passages. The C4-2B-ENZR cell lines were established as described previously [21]. The LNCaP-ENZR cell line was developed by long-term culture at a concentration of 10 μM enzalutamide for over 6 months. We conducted thorough experimental verification to confirm that the resistance phenotype had been established. Enzalutamide (E120461), EG01377 (T72276), and perifosine (S1037) were procured from Energy Chemcial.

Cell transfection

PLXNA1 and AR expression vectors were synthesized by Biosune Biotech. Ribobio provided all siRNA sequences and negative controls. The pCMV shPLXNA1 plasmid, along with packaging and envelope plasmids, were co-transfected into 293T cells. This process generated the PLXNA1 shRNA lentiviral particles, which were subsequently harvested, stored at -80°C, and utilized for later transduction of PCa. We then constructed PCa ENZR cell lines with stable shRNA knockdown of PLXNA1. Detailed information on the specific target sequences were provided in **Supplementary Table 3.**

Cell viability assays

We used the MTS Kit (BestBio) to measure cell viability. The cells treated according to different experimental purposes were seeded in 96-well plates. MTS was added at relevant experimental time points, and after incubating at 37°C for 2 hours, absorbance was measured. The colony formation assay was used to assess cell clonogenic capacity. The treated cells were seeded in 6-well plates, treated with respective drugs, fixed, stained, and counted after approximately 15 days. Experiments were independently replicated three times.

Immunofluorescence (IF)

For immunofluorescence analysis, 4 μm tissue sections were fixed and stained with antibodies against PLXNA1 (1:100, Abcam, ab217634) and NRP1 (1:100, Proteintech, 60067-1-Ig). The sections were then treated with fluorescent secondary antibodies, followed by DAPI staining for nucleus visualization. Finally, we used a confocal microscope for observation and image acquisition.

RNA extraction

The cells were lysed with an appropriate amount of Trizol (Invitrogen), and mRNA was extracted according to the experimental procedure. The primer sequences were provided in **Supplementary Table 4**.

Apoptosis detection

PCa cell lines with ENZR were transfected with siPLXNA1 and then treated for 48 hours. Apoptosis was assessed using an annexin V-FITC/propidium iodide (PI) staining kit (C1062, Beyotime, China), following the manufacturer's protocol. The distribution of cells at various stages of apoptosis was then analyzed using a Beckman Coulter FC500 flow cytometer (Brea, CA). The data were processed with FlowJo software.

Chromatin immunoprecipitation (ChIP)

Chromatin from pretreated cells was fixed with 1 % formaldehyde for 11 minutes. DNA was fragmented into 200-500 bp fragments using a sonicator (10^6 cells in 500 μL volume; ultrasound 15s, stop 9s, repeated five times). Immunoprecipitation of chromatin was conducted using anti-AR antibodies (Abcam, Cambridge, MA, USA) and anti-IgG antibodies (St. Louis, MO, USA). The enrichment of AR within PLXNA1 promoter was assessed by RT-qPCR using chromatin immunoprecipitated from cells with the indicated primers listed in **Supplementary Table 4**.

In vivo study

All animal experiments adhered to the experimental animal welfare and ethics regulations of Qilu Hospital, Shandong University. Male nude mice (nu/nu) were injected with C4-2B, C4-2B-ENZR, C4-2B-ENZR-shNC, or C4-2B-ENZR-shPLXNA1 cells (3×10^6) at 5 weeks of age. When tumors reached a certain volume, mice bearing C4-2B-ENZR tumors were randomly assigned to four groups (n = 5-6): control (DMSO), enzalutamide (10 mg kg^{-1}), perifosine (100 mg kg^{-1}), or combination

therapy. Tumor growth was monitored every 2-5 days until mice were sacrificed, with tumor sizes serving as the primary measure of response. The mice in the other groups were treated individually with enzalutamide. Our research has been approved by an ethical committee that adheres to the principles of the Basel Declaration.

Bioinformatics analysis

We obtained datasets from the GEO database (https://www.ncbi.nlm.nih.gov/geo/), including GSE48403, GSE51873, GSE126881, GSE78201, GSE44905, GSE64143, GSE8511, GSE6752, GSE6919, GSE23451, GSE29079, GSE70769, GSE46602, and GSE141551 [22-32]. ChIP-seq data of AR in PCa cells was downloaded from GEO database as GSM2058879, GSM1501185 and GSM1586660, respectively [33,34]. The visualization of ChIP-seq data was performed with UCSC browser. The SU2C 2019 dataset was downloaded from cBioPortal (http://www.cbioportal.org). The gene expression data was analyzed for enrichment of biological themes using Gene Set Enrichment Analysis (GSEA) (https://www.gsea-msigdb.org/gsea/login.jsp) [35,36]. We explored the relationship between PLXNA1 expression and disease-free survival in PCa cases using the GSE46602 and GSE70769 datasets.

Western blotting

Western blotting was performed following previously described procedures [21]. Co-IP assays were carried out following the instructions provided with the Pierce™ Co-IP Kit (Thermo, cat no 26149). The resulting immuno-complexes were collected and subsequently analyzed using western blotting. Primary antibodies utilized in the western blotting assays are listed in **Supplementary Table 5**.

Fluorescence resonance energy transfer (FRET)

To detect protein-protein interactions, we conducted FRET experiments. 293T cells were transfected with sensor pairs plasmids, comprising cyan fluorescent protein (CFP)-PLXNA1 and yellow fluorescent protein (YFP)-NRP1, and cultured on glass coverslips for 24 hours. Following the incubation period, cells were treated with 4 % paraformaldehyde and subjected to immunocytochemistry. Histogram data representing mean FRET efficiency were generated from analysis of $>$ 15 cells per sample. Each experimental trial was conducted independently and repeated a minimum of three times.

Molecular docking

The crystal structures of PLXNA1 (protein ID: Q9UIW2) and NRP1 (protein ID: O14786) were retrieved from the AlphaFold database (https://alphafold.com). The central coordinates for docking were determined using GRAMM Docking (https://gramm.compbio.ku.edu), followed by virtual molecular docking using AutoDock Vina. The optimal binding pose was visualized using PyMOL (version 2.5.7) to generate the docking image.

Statistical analysis

The experiments were independently repeated at least three times, producing consistent results. Numerical data are presented as mean ± SD and were assessed for normality using Shapiro-Wilk test and visually using both histograms and boxplots. Categorical data are expressed as number (%). If the data followed a normal distribution, we used Student's t-test for analysis. Otherwise, Mann-Whitney U test was used. Survival analysis employed the Kaplan-Meier method with Log-rank tests. Statistical analyses were conducted using GraphPad Prism 9 software (RRID: SCR_002798), and correlations were assessed with either the Chi-Square Test or Fisher's exact test. Tumor growth data were analyzed using the ANOVA method, with statistical significance defined as $P < 0.05$.

Results

Elevated PLXNA1 expression correlates with enzalutamide resistance in PCa cells

Overexpression of PLXNA1 has been demonstrated to correlate with advanced pathological staging and poor survival outcomes in primary PCa [18]. Firstly, we verified the phenotype of the enzalutamide-resistant cell lines (*Supplementary Fig. 1A-B*). Of interest, PLXNA1 expression was found to be significantly higher in ENZR cells compared to parental cells (*Fig. 1A*). Bioinformatics analysis also showed that higher mRNA expression of PLXNA1 was observed in ENZR xenograft (*Fig. 1**B left panel***) and enzalutamide treated cells (*Fig. 1**B right panel***) of PCa. To support this notion, we constructed Parental/ENZR xenografts with nu/nu mice to investigate the PLXNA1 expression *in vivo*. The IHC result revealed increased PLXNA1 expression in ENZR xenografts in compare with that of the parental tumors (*Fig. 1**C***). Moreover, prolonged enzalutamide treatment (~3 months) in PCa cells resulted in augmented PLXNA1 expression (*Fig. 1**D-E***). Bioinformatics analysis revealed the top 5 enriched signaling pathways altered after androgen ablation, including the axon guidance pathway, which involves the role of PLXNA1. This suggested that PLXNA1 may be associated with the failure of ADT (*Fig. 1**F***). Bioinformatic analysis revealed the positive correlation between axon guidance pathway and pathways that were elevated in CRPC and ENZR [9,37], in PCa, and in pan-cancer setting as well (*Fig. 1**G***). Noteworthy, among the receptors within the axon guidance pathway, only PLXNA1 showed increased levels after enzalutamide treatment in VCaP cells (*Fig. 1**H***). This collective data demonstrated a heightened expression of PLXNA1 in PCa with ENZR.

PLXNA1 contributes to ENZR and promote ENZR tumor progression

To explore the involvement of PLXNA1 in ENZR development, we performed PLXNA1 knockdown in ENZR cells and overexpression in parental cells (***Supplementary Fig. 2A-B***). Following incubation with 20 μM enzalutamide for 4 days, PLXNA1 depletion in ENZR cells augmented the inhibitory impact of enzalutamide on cell growth (*Fig. 2**A-B***). Conversely, overexpression of PLXNA1 in parental cells appeared to rescue cells from enzalutamide-induced growth inhibition (*Fig. 2**C-D***). The inhibitory effect of enzalutamide on cells is neutralized in the presence of DHT. Similar trends were observed in anchorage-independent colony formation assays. Upon exposure to enzalutamide, cells with PLXNA1 knockdown displayed a notable reduction in the colony number (*Fig. 2**E-F***). Conversely, heightened PLXNA1 expression amplified the colony formation capacity, leading to increased numbers and sizes of colonies (*Fig. 2**G-H***). In addition, PLXNA1 knockdown in ENZR cells increased, whereas PLXNA1 overexpression in parental cells reduced the sensitivity to enzalutamide (*Fig. 2**I-J***). Knockdown of PLXNA1 in ENZR cells also led to a slight increase of apoptosis as measured by flow cytometry (***Supplementary Fig. 2C-E***). Additionally, suppression of PLXNA1 in C4-2B-ENZR xenografts significantly decreased tumor growth. The mean tumor volume was 307.5 mm^3 in PLXNA1 knockdown xenografts, compared to 1477.3 mm^3 in the control group (*Fig. 2**K, Supplementary Fig. 2F***). In the meantime, a significant decrease in average tumor weight (0.36 g vs. 1.24 g) and reduced cell proliferation, assessed by Ki67 IHC, were also observed in PLXNA1 knockdown xenograft (*Fig. 2**L-M, Supplementary Fig. 2G-H***). Collectively, these results provided compelling evidence that PLXNA1 confers survival advantage to PCa cells under enzalutamide treatment, thereby facilitating ENZR tumor progression.

AR directly repressed PLXNA1 gene transcription

To determine whether PLXNA1 is an androgen regulated gene, we initially demonstrated that both PLXNA1 mRNA and protein levels exhibited a significant decrease upon DHT treatment (*Fig. 3**A-C***). AR

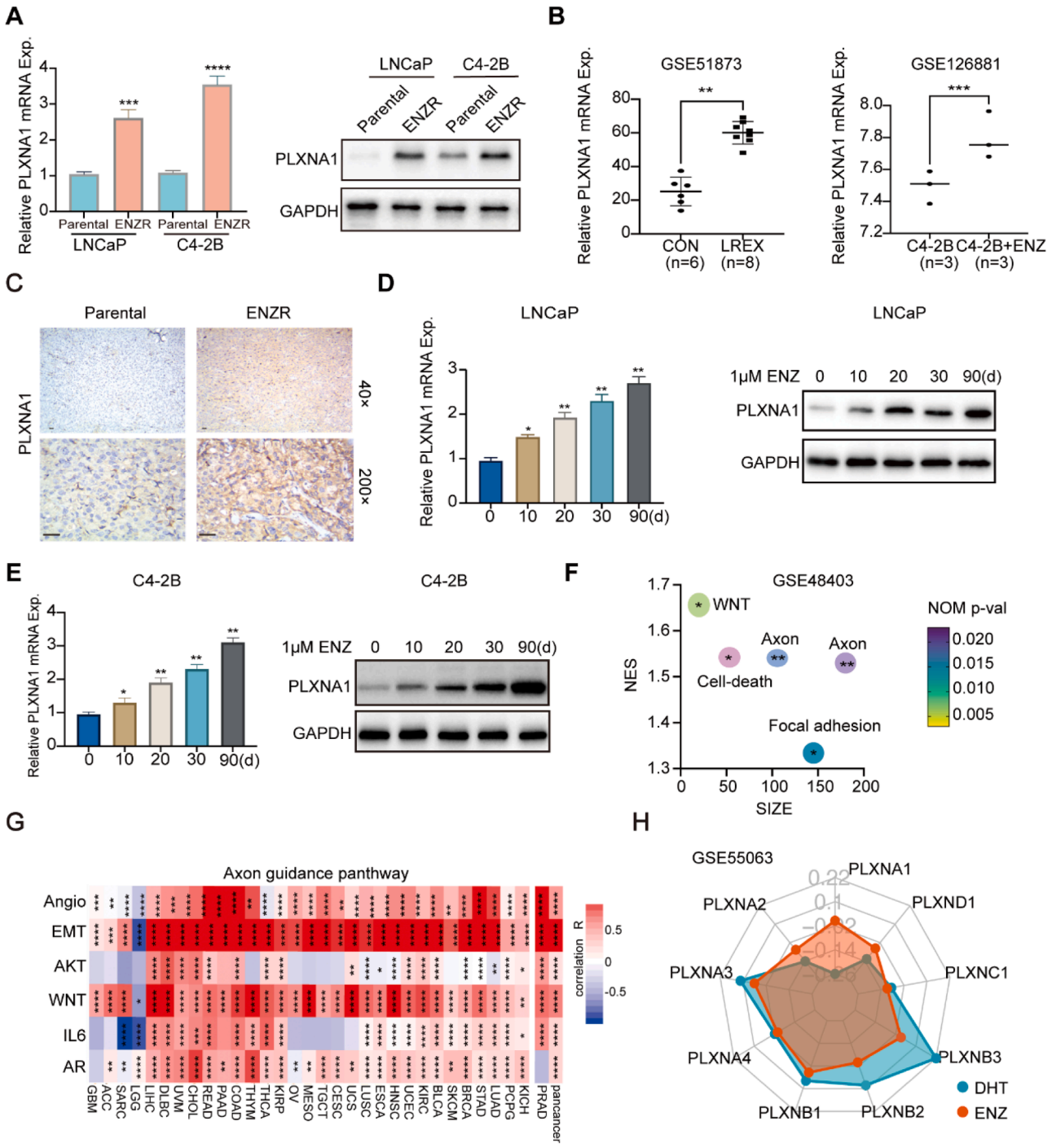

Fig. 1. Identification of PLXNA1 high expression in enzalutamide resistant PCa.
(A) The expression of PLXNA1 in previously constructed enzalutamide sensitive and resistant LNCaP and C4-2B cells. RT-qPCR and western blotting assays were used to assess mRNA level (left) and protein level (right), respectively. (B) PLXNA1 expression in the public datasets of GSE51873 and GSE126881. The assessment included PLXNA1 expression in enzalutamide-sensitive (con) and resistant (LREX) xenografts (left panel), as well as in vehicle-treated and enzalutamide-treated C4-2B cells (right panel) (Mann-Whitney U test). (C) Representative images of IHC staining of PLXNA1 in tumor sections isolated from enzalutamide sensitive and resistant xenograft. Scale bar, 50 μm. (D-E) The mRNA level and protein level of PLXNA1 during prolonged enzalutamide treatment of LNCaP and C4-2B cells. LNCaP and C4-2B cells were treated with 1 μM enzalutamide for 0–90 days. PLXNA1 mRNA and protein levels were detected at the indicated time points by RT-qPCR and western blotting. (F) The top KEGG pathways enriched ($P<0.05$) in androgen-deprivation therapy-resistant tumors in GSE48403 datasets. (G) The correlation heatmap describing the association between axon guidance pathway and multiple cancer hallmarks in pan-cancer using the z-score algorithm. (H) The radar charts showing the expression levels of axon guidance receptors in VCaP cells treated with dihydrotestosterone or enzalutamide according to GSE55063 data. ENZ, enzalutamide. d, days; DHT, Dihydrotestosterone; ENZ, enzalutamide; CON, Mice were then treated with vehicle; LREX, LNCaP Resistant to Enzalutamide Xenograft Derived; Angio, angiogenesis. Data are represented as mean ± SD of three independent experiments. The data were assessed for normal distribution using the Shapiro-Wilk test. The two-sided Student's t-test was utilized for comparing differences among these variables. *$P<0.05$, **$P<0.01$, ***$P<0.001$.

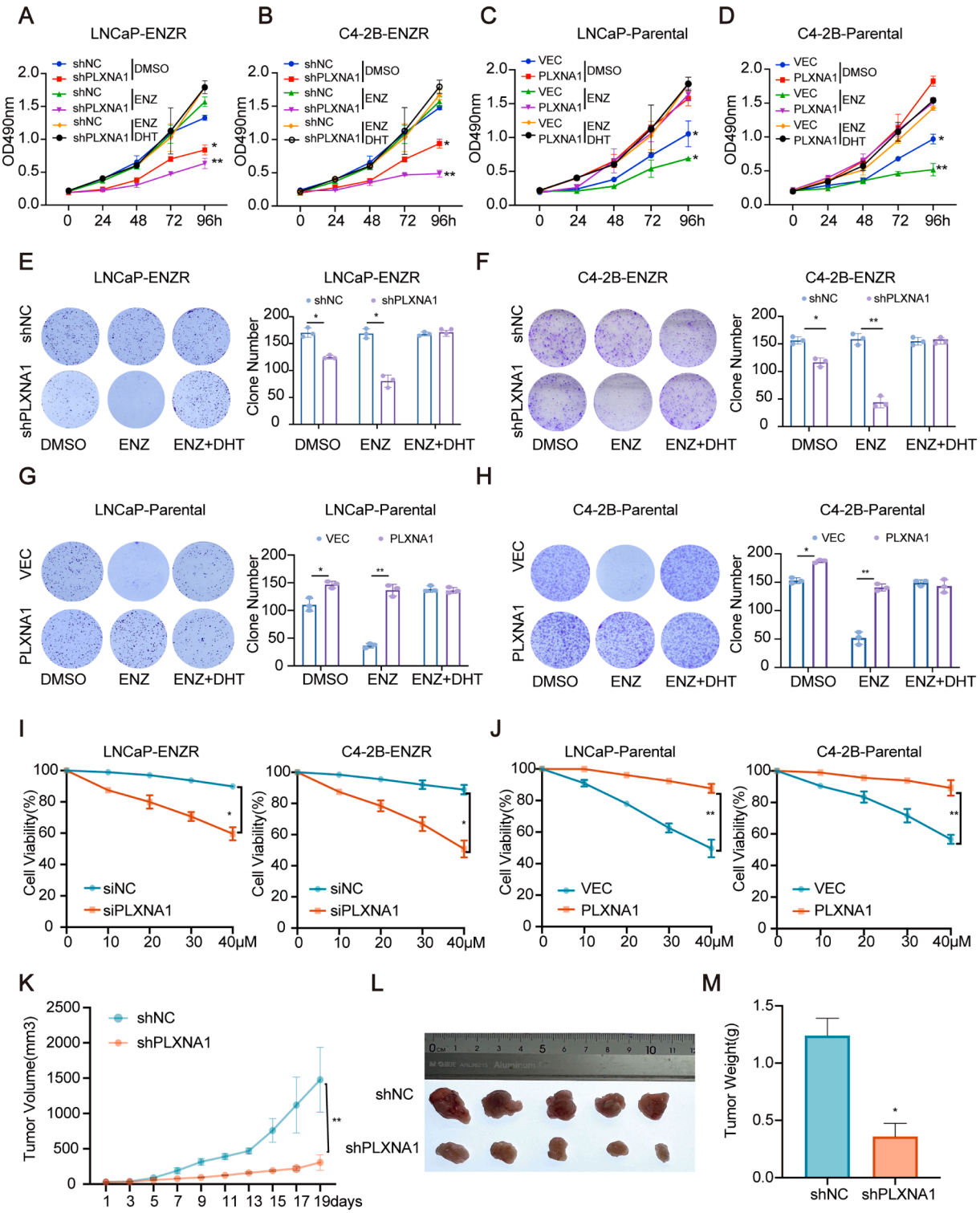

Fig. 2. PLXNA1 promotes cell growth.

(A-H) Cell proliferation assessed by MTS assay and colony formation assay in indicated cells. LNCaP-ENZR and C4-2B-ENZR cells were transfected with shNC or PLXNA1 shRNA (shPLXNA1, stable transfection) and LNCaP-Parental and C4-2B-Parental cells were transfected with empty vector (VEC) or PLXNA1 overexpression plasmid (PLXNA1). For colony formation assays, colonies containing >50 cells were counted and plotted. Quantitative analysis of colony numbers was shown in the right panel. ENZ, 20 μM enzalutamide; DHT, 10nM DHT. (I-J) Cell viability measured by MTS assay in the indicated cell lines under enzalutamide treatment. LNCaP-ENZR, C4-2B-ENZR (I), and LNCaP-Parental, C4-2B-Parental (J) cells were transfected as indicated and treated with titrated doses of enzalutamide for 3 days. (K-M) Effect of PLXNA1 knockdown on tumorigenesis *in vivo* evaluated with ENZR xenografts model. C4-2B-ENZR cells with stable knockdown of PLXNA1, as well as their parental controls, were subcutaneously injected into nude mice (n = 5/group). The tumor volume was measured every two days after nude mice were castrated (K). Tumors were isolated from mice, photographed, and weighed at the endpoint (L, M). Data are represented as mean ± SD of three independent experiments. The data were assessed for normal distribution using the Shapiro-Wilk test. The two-sided Student's t-test was utilized for comparing differences among these variables. **P*<0.05, ***P*<0.01, ****P*<0.001.

silencing in LNCaP and C4-2B cells led to elevated PLXNA1 levels (*Fig. 3**D-E***), whereas exogenous AR suppressed PLXNA1 expression in PC3 and DU145, which were AR-negative cell lines (*Fig. 3**F-G***). Interrogation of publicly available data revealed chromatin binding of AR in PLXNA1 promoter region across three PCa cell lines (*Fig. 3**H***). Using JASPAR and the PROMO database, we identified a potential AR binding site. ChIP-qPCR assays confirmed AR recruitment to the PLXNA1 region in LNCaP and ENZR cells, which was decreased with enzalutamide treatment (*Fig. 3**I***). Our studies collectively demonstrated that AR directly represses PLXNA1 transcription through recruitment to the PLXNA1 promoter.

PLXNA1 enhances ENZR by activating AKT signaling pathway in PCa cells

The aforementioned data (*Fig. 1**G***) displayed the potential for crosstalk between axon guidance pathway and AKT pathway, but no significant correlation with AR pathway in PCa. Therefore, we hypothesized that PLXNA1 may active AKT signaling pathway to promote ENZR. As indicated, phosphorylated AKT (p-AKT) was significantly elevated in both ENZR cells and ENZR xenografts, exhibiting a similar trend as PLXNA1 (*Fig. 4**A-C***). Moreover, depletion of PLXNA1 reduced (*Fig. 4**D left panel***), whereas PLXNA1 overexpression intensified the phosphorylation levels of AKT (*Fig. 4**D right panel, Supplementary Fig. 3A***). Furthermore, GSEA analysis unveiled a notable enrichment of the AKT signaling pathway linked to elevated PLXNA1 expression in ENZR PCa cells (*Fig. 4**E-F***). To further validate the correlation between PLXNA1 and AKT signaling in ENZR development, we treated PLXNA1-altered cells with AKT inhibitor, perifosine. Perifosine reduced AKT phosphorylation in ENZR cells (***Supplementary Fig. 3B-C***). PLXNA1 overexpression enabled sustained proliferation of LNCaP and C4-2B cells in presence of enzalutamide, which was counteracted by perifosine treatment (*Fig. 4**G***). Moreover, the viability of ENZR cells could be compromised either by silencing PLXNA1 or by treatment with perifosine (*Fig. 4**H***). Overexpression of PLXNA1 in parental cell lines can increase the phosphorylation of AKT protein, and this increase can be blocked by perifosine (*Fig. 4**I***). Additionally, the enhanced cell proliferation induced by PLXNA1 overexpression can also be blocked by perifosine (*Fig. 4**J***). To fulfill the crosstalk between axon guidance pathway and AKT signaling pathway, the ligand of PLXNA1, Semaphorin-3a (Sema3A), was investigated.

The activation of the AKT signaling pathway by Sema3A could be inhibited by PLXNA1 knockdown (***Supplementary Fig. 4A-B***). However, the phosphorylation of AKT induced by PLXNA1 expression was not diminished in absence of Sema3A (***Supplementary Fig. 4C-D***). Taken together, PLXNA1 serves as a pivotal mediator in coordinating the crosstalk between the axon guidance pathway and the AKT signaling pathway in ENZR.

PLXNA1 activates AKT signaling pathway by recruiting NRP1

NRP1 is a transmembrane glycoprotein receptor known to mediate signaling within the axon guidance pathway [38]. Zhang et. al have documented NRP1′s involvement in activating AKT in response to EGFR stimulation [39]. Additionally, ENZR PCa cells had more NRP1 protein compared to the parental cells (***Supplementary Fig. 5A***). To investigate whether NRP1 participated in PLXNA1-induced AKT phosphorylation, we inhibited NRP1 using either siRNA or a small-molecule inhibitor, EG01377. Western blotting results revealed that the inhibition of NRP1 resulted in decreased phosphorylation of AKT in the presence of PLXNA1 overexpression, suggesting NRP1′s contribution to PLXNA1-mediated AKT activation. (*Fig. 5**A-B***). We observed that EG01377 blocked PLXNA1 induced phosphorylation of PDK1, the direct kinase of AKT phosphorylation, acts as a master kinase in AKT signaling pathway by phosphorylation of AKT at T308 [40]. Co-IP assays revealed that PLXNA1 interacts with NRP1 in ENZR cells (*Fig. 5**C***). Co-localization of PLXNA1 and NRP1 was further confirmed with confocal immunofluorescence (*Fig. 5**D***). Significantly, the interaction between PLXNA1 and NRP1 was notably stronger in ENZR cells than in parental cells (*Fig. 5**E***). To determine whether PLXNA1 and NRP1 directly bind to each other, we have applied pb-FRET analysis. The results showed direct binding between these two proteins (*Fig. 5**F left panel***). Moreover, treatment with EG01377 decreased the interaction between PLXNA1 and NRP1 (*Fig. 5**F right panel***). To identify the key region of PLXNA1 involved in the interaction with NRP1, Co-IP assays were conducted using three truncated NRP1 constructs (*Fig. 5***G, *Supplementary Fig. 5B***). The Co-IP analysis showed that PLXNA1 interacted with both the NRP1-CUB and NRP1-MAM domains, underscoring the significance of the b domain of NRP1 in facilitating this interaction (***Supplementary Fig. 5C***). Additionally, the protein molecular docking model supported this observation (*Fig. 5**H***). Treatment with NRP1 inhibitor, EG01377, disrupt the complex of PLXNA1-NRP1, and further recruitment of PDK1 by NRP1 as well (***Supplementary Fig. 5D-E***). As shown in ***Supplementary Fig. 5F-G***, co-treatment with EG01377 remarkably reduced the IC50 values for enzalutamide in ENZR cells. These findings implied that PLXNA1 may activate the AKT signaling pathway by engaging NRP1.

AKT inhibition suppresses ENZR PCa cell growth and xenograft tumor progression

We then examined if perifosine could enhance enzalutamide efficacy in ENZR PCa cells. ENZR cells were exposed to DMSO, enzalutamide, perifosine, or a combination of enzalutamide and perifosine. As shown in *Fig. 6**A*** and *Fig. 6**B***, perifosine alone showed growth inhibitory effects, which were notably strengthened when combined with enzalutamide. To validate the synergistic effect of perifosine and enzalutamide, we assessed the half-maximal inhibitory concentration (IC50). As shown in *Fig. 6**C-D***, co-treatment with perifosine remarkably reduced the IC50 values for enzalutamide in LNCaP-ENZR (119.7μM vs. 42.8μM) and C4-2B-ENZR cells (122.2μM vs. 38.1μM). Combined treatment of enzalutamide with perifosine in ENZR cell lines resulted in substantial dose-dependent growth inhibition of enzalutamide, as well as reduction in clone numbers assessed by colony formation assays (*Fig. 6**C-E***). The combination of enzalutamide and perifosine exhibited synergy effect in vitro (*Fig. 6**F-G, Supplementary Fig. 6A-B***). To assess synergistic effects *in vivo*, we used ENZR xenograft models in nude mice. Enzalutamide alone modestly decreased tumor weight, while combining enzalutamide with perifosine substantially reduced both tumor size and weight (*Fig. 6**H-I***), as well as reduction in cell proliferation index, Ki67 (*Fig. 6**J-K***). No anomalies in the function or histology of major visceral organs were detected (***Supplementary Fig. 6C***). Treatment with the combinatorial regimen (enzalutamide plus perifosine) also induced the decrease of phosphorylation level of AKT (***Supplementary Fig. 6D***). These results imply that incorporating an AKT inhibitor alongside enzalutamide treatment could heighten the responsiveness of prostate tumors, thereby advocating for the combination therapy in managing patients with CRPC (*Fig. 6**L***).

PLXNA1 overexpression predicts poor prognosis in PCa

Ren et al. demonstrated that approximately 23 % of primary PCa cases from Chinese patients exhibited commonly dysregulation of axon guidance pathway genes through gain/amplification or overexpression [18]. We also found PLXNA1 amplification in CRPC and primary PCa patients from western populations, with elevated proportion in CRPC (*Fig. 7**A-B***). GSEA analysis identified AKT signaling enrichment in both CRPC and primary PCa patients with PLXNA1 amplification, indicating potential clinical implications for AKT inhibitor in this subgroup (*Fig. 7**C-D***).

Increased PLXNA1 expression was positively corelated with PLXNA1 copy number and were observed consistently in metastatic CRPC patients across various cohorts (***Supplementary Fig. 7A-E***). For further validate the clinical significance of PLXNA1 in PCa, IHC was performed

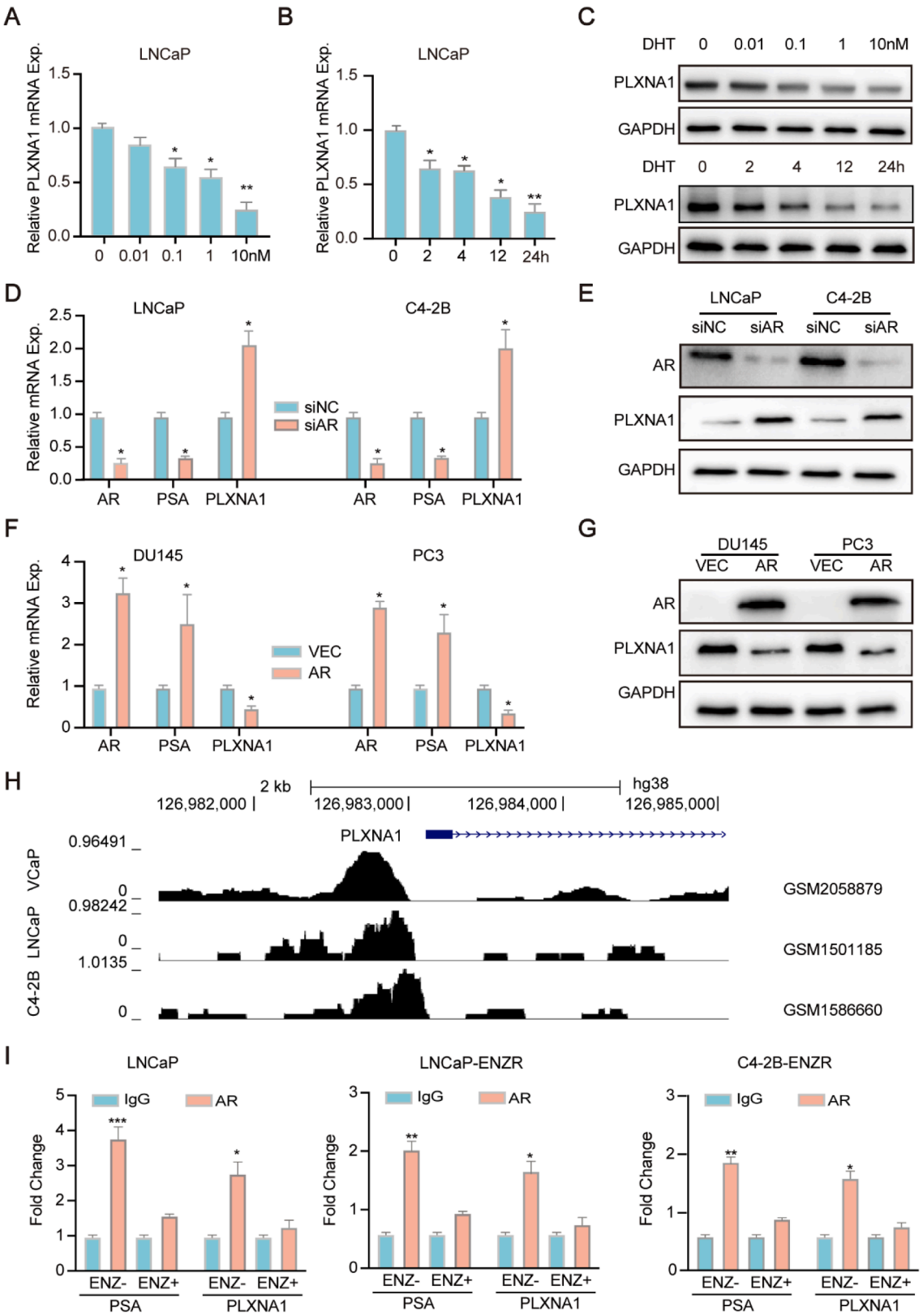

Fig. 3. PLXNA1 is an AR repressed gene.

(A-C) Androgen responsiveness of PLXNA1 in PCa cells. LNCaP cells were cultured in CS-FBS medium for 4 days before challenged with 0-10 nM DHT for 24 h or 1 nM DHT for 0-48 h. The mRNA and protein expression levels of PLXNA1 were measured by RT-qPCR and western blotting assays. DHT, dihydrotestosterone; h, hours. (D-G) RT-qPCR (D, F) and western blotting (E, G) analysis of AR, PLXNA1 and PSA in PCa cells that were treated with AR siRNA or AR expression plasmid. siNC, small interfering Negative Control; VEC, vector. (H) Analysis of ChIP-seq data from VCaP cells (GSM2058879), LNCaP cells (GSM1501185) and C4-2B cells (GSM1586660) showing AR enrichment in PLXNA1 promoter region. (I) ChIP-qPCR analysis of AR recruitment onto the PLXNA1 promoter in LNCaP, LNCaP-ENZR and C4-2B-ENZR

cells. Purified rabbit IgG was used as a negative control. Primers covering the AR binding site on the PSA gene promoter were used as positive controls. Data are represented as mean ± SD of three independent experiments. *P<0.05, **P<0.01, ***P<0.001.

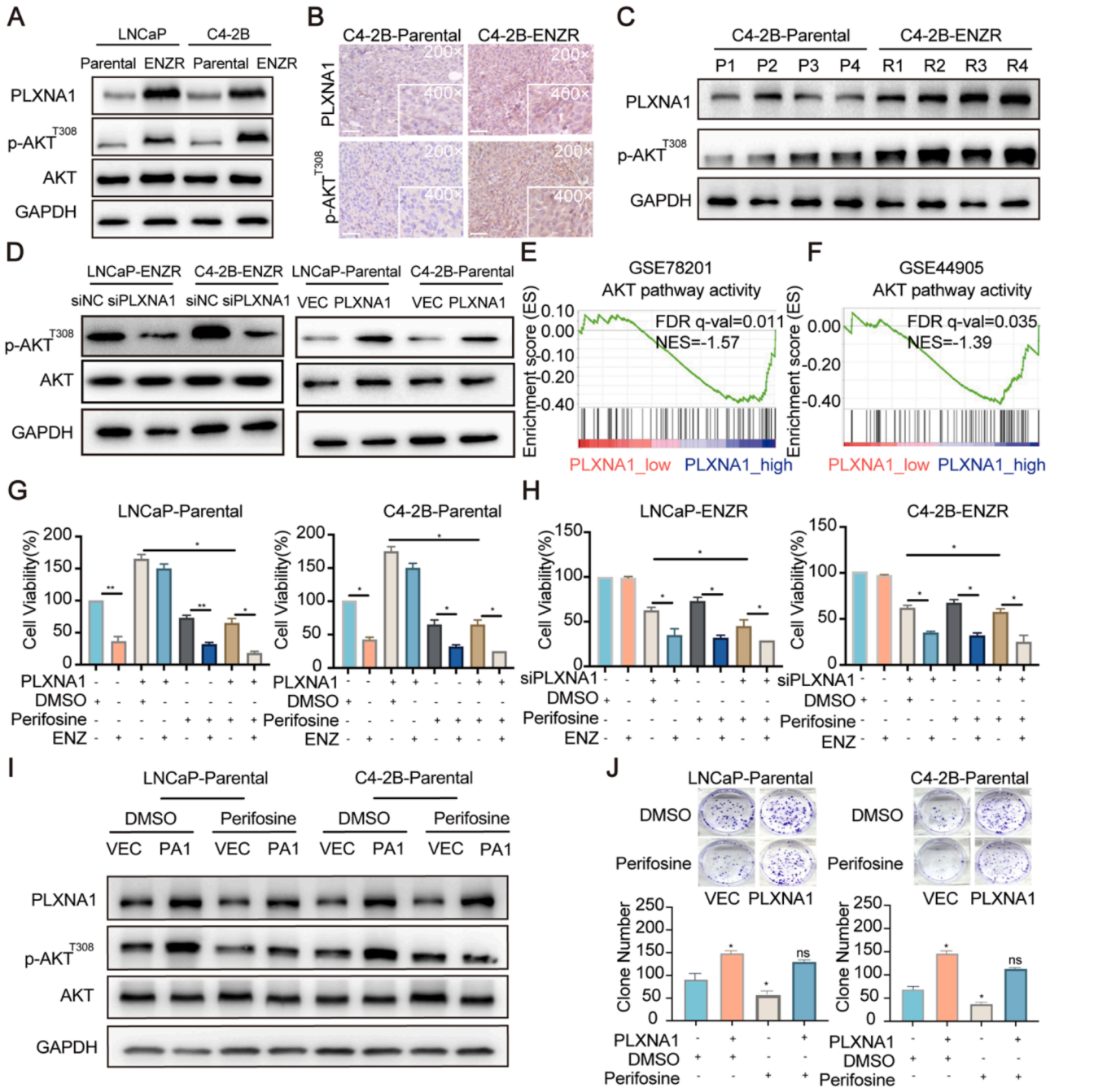

Fig. 4. PLXNA1 activates AKT signaling to promote the enzalutamide resistance.
(A) Immunoblots of indicated proteins in LNCaP-Parental/LNCaP-ENZR and C4-2B-Parental/C4-2B-ENZR cells. (B) Representative images of IHC staining of PLXNA1 and p-AKT in tumor sections isolated from xenograft mice. Representative cases of PLXNA1 (upper panel) or and p-AKT (lower panel) staining are shown. (C) Western blotting results showing PLXNA1 and p-AKT expression in four enzalutamide sensitive (P1-4) and four resistant (R1-4) xenograft samples. (D) Immunoblots showing phosphorylation level of AKT in indicated cells. LNCaP-Parental, C4-2B-Parental, LNCaP-ENZR and C4-2B-ENZR cells were transfected with indicated plasmid or siRNA. Cells were then collected and analyzed by western blotting. (E-F) Enrichment of AKT-mediated gene program analyzed by GSEA. GSEA analysis was performed to determine the enrichment of AKT downstream target gene set in gene expression dataset profiling PLXNA1_low and PLXNA1_high in GSE78201 as well as GSE44905. NES, normalized enrichment score. (G-H) Cell viability was measured in the indicated cell lines under AKT pathway inhibitor perifosine or enzalutamide treatment. (I) Western blotting analysis of phosphorylation level of AKT in indicated cells with or without perifosine treatment. LNCaP-Parental and C4-2B-Parental cells were transfected with indicated plasmid or PLXNA1 under AKT signaling pathway inhibitor perifosine or DMSO treatment. (J) Clonal assay of indicated cells with or without perifosine treatment. Representative images (upper panel) and quantification (lower panel) were presented. Data are represented as mean ± SD of three independent experiments. The two-sided Student's t-test was utilized for comparing differences among these variables. *P<0.05, **P<0.01, ***P<0.001.

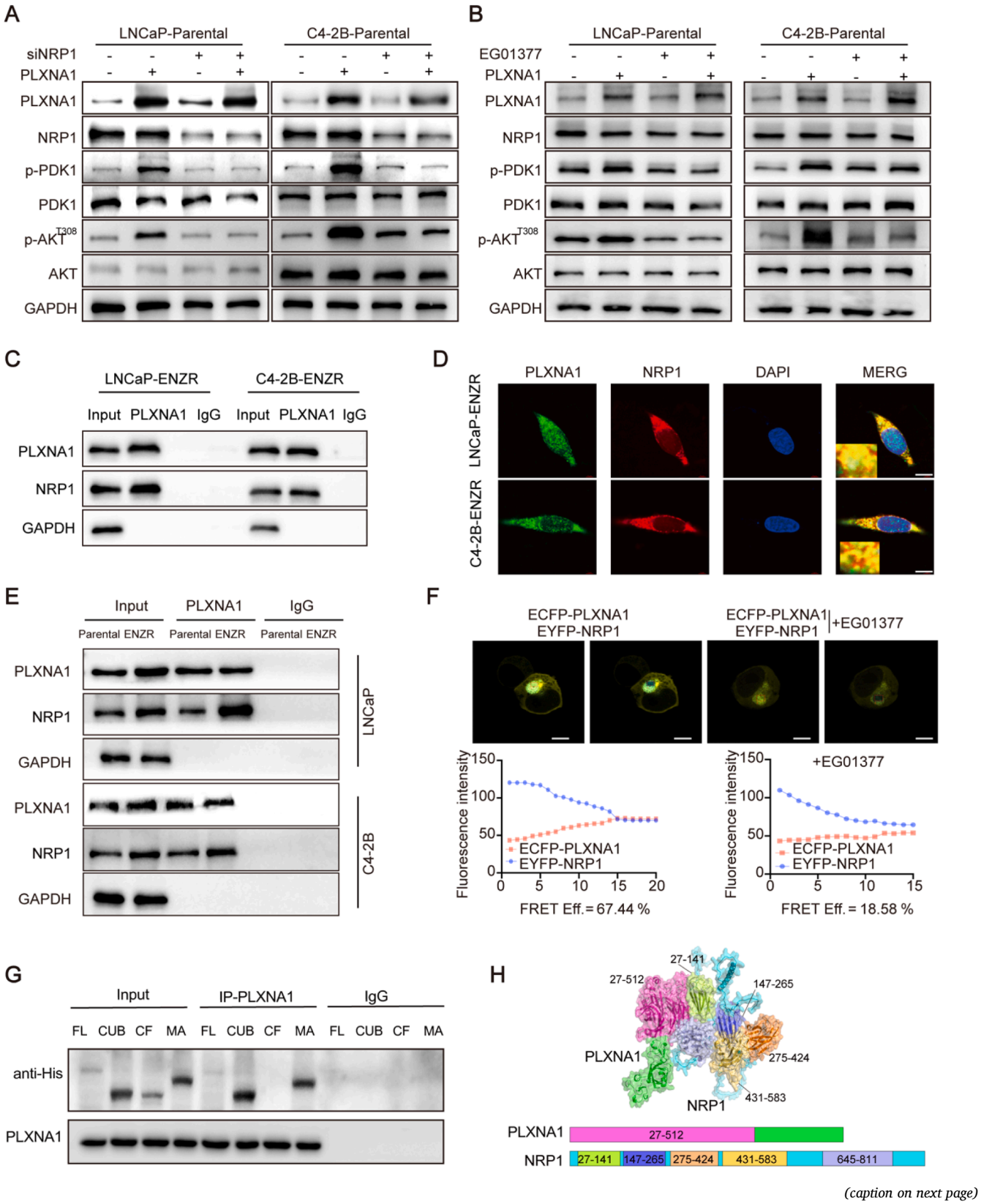

(caption on next page)

Fig. 5. PLXNA1 activates AKT signaling pathway through the recruitment of NRP1.
(A) Immunoblots of indicated proteins in LNCaP-Parental and C4-2B-Parental cells. The cells were transfected with indicated plasmid or siRNA. Cells were then collected and analyzed by western blotting. (B) Immunoblots of indicated proteins in LNCaP-Parental and C4-2B-Parental cells. The cells were transfected with PLXNA1 plasmid or EG01377. Cells were then collected and analyzed by western blotting. (C) Immunoblots of Co-IP assays showing interaction between PLXNA1 and NRP1. Co-IP assays were performed using LNCaP-ENZR and C4-2B-ENZR cell lysates. (D) Immunofluorescence staining showing PLXNA1 (green) and NRP1 (red) localizations in LNCaP-ENZR and C4-2B-ENZR cells. All pictures were imaged using a confocal microscope. Representative images are shown with a 10 μm scale bar. Boxes represent regions in higher magnification. (E) Co-IP assays of PLXNA1 and NRP1 were performed using LNCaP-Parental/ENZR and C4-2B-Parental/ENZR cell lysates. (F) Representative FRET measurement illustrating interaction of PLXNA1 and NRP1 in 293T cells. FRET was performed to examine the 293T cells were co-transfected with plasmids of FRET sensor pairs cyan fluorescent protein (CFP)-Donner (PLXNA1) and yellow fluorescent protein (YFP)-Acceptor (NRP1). Fluorescence intensity were detected using a confocal microscope. Representative images are shown with a 10 μm scale bar (top). The fluorescence intensity of CFP and YFP channels before and during acceptor photobleaching (bottom). All pictures were imaged using a confocal microscope (63 ×). (G) Immunoblots of Co-IP assays showing interaction between PLXNA1 and NRP1. Co-IP assays were performed using C4-2B-ENZR cell lysates. (H) Molecular docking analysis shows the interaction domain between PLXNA1 and NRP1. Data are represented as mean ± SD of three independent experiments. The two-sided Student's t-test was utilized for comparing differences among these variables. $^{*}P<0.05$, $^{**}P<0.01$, $^{***}P<0.001$.

on a total of 171 PCa samples, including 142 primary PCa and 29 CRPC. Out of the 142 patients with primary PCa, 80 individuals (56.34 %) exhibited either negative or weak staining, while 62 individuals (43.66 %) demonstrated moderate or strong cytoplasmic staining for PLXNA1. Nonetheless, within the subset of 29 CRPC patients, 6 individuals (20.69 %) exhibited negative or weak staining, and 23 individuals (79.31 %) displayed moderate or strong cytoplasmic staining for PLXNA1. The IHC results validated elevated PLXNA1 expression in CRPC (*Fig. 7**E-F***). Of significance, patients with elevated PLXNA1 expression exhibited decreased disease-free survival rates (*Fig. 7**G-I***).

Discussion

We found upregulated expression of PLXNA1 in ENZR PCa, and overexpression of PLXNA1 conferred robust acquired drug resistance. Mechanistically, PLXNA1 recruited NRP1 forming a PLXNA1-NRP1 complex, which in turn potentiated the phosphorylation of the AKT. Perifosine, an AKT inhibitor, was able to reinstate the inhibitory effect of ENZR cells. Additionally, combined therapy using an AKT inhibitor and enzalutamide effectively overcome PLXNA1-induced ENZR. Therefore, our findings hold promising translational potential and benefit patients suffering with ENZR PCa.

PLXNA1, acting as a receptor for SEMA3A in the axon guidance pathway, plays a multifaceted role in various aspects of nervous system development, ranging from neuron migration and polarization, synaptogenesis to energy homeostasis and glucose homeostasis [41,42]. The role of PLXNA1 in cancer remains incompletely understood, but various mechanisms have been proposed. Though binding to SEMA3A, PLXNA1 counteract the anti-angiogenic properties of SEMA3A, thereby stimulating angiogenesis—an event that supports tumor progression and metastasis [42,43]. In addition, there are studies reporting that SEMA3C/PlexinA2/NRP1 promotes perineural invasion of PCa cells [44]. This similarity to our research findings strengthens the credibility of our study and provides broader background support. Zhang et al. discovered that NRP1 facilitates the aggressiveness of PCa by triggering the AKT signaling pathway through EGFR activation [39]. Further exploration in this field will advance our comprehension of PCa development and treatment strategies. The interactions between PLXNA1 and other cytokine receptors, notably VEGFR2 and EGFR, have the potential to trigger downstream signaling pathways, thereby fostering tumor growth and metastasis [45].

Additionally, research has shown that PLXNA1 facilitates cell migration and invasion in breast cancer and PCa cells, potentially through its interaction with the extracellular matrix and the activation of signaling pathways such as the Rho family of GTPases [46]. Our findings uncovered a significant correlation between elevated PLXNA1 expression and the acquisition of ENZR, thus linked to a poorer prognosis in PCa. The aberrant expression of PLXNA1 appears to constitute a plausible mechanism contributing to the failure of hormonal treatments.

Resistance to ADT can arise via various mechanisms, including genomic alterations of the AR, acquisition of linage plasticity, activation Wnt-β-catenin pathway and AKT pathway, etc. [47-50]. In PTEN-deficient PCa, amplified AKT signaling and a reciprocal feedback loop with AR signaling synergistically promote cell survival [51]. Notably, the activation of the AKT signaling pathway, independent of Receptor Tyrosine Kinases (RTKs), may derive from alternative intracellular signaling pathways or cytokine receptors, including G-protein coupled receptors [52]. The present study has clarified the interplay between the axon guidance pathway and the AKT signaling pathway, with a particular focus on the involvement of PLXNA1 in triggering the activation of the AKT signaling pathway in ENZR. PLXNA1 activates the AKT signaling pathway through recruitment of NRP1 and further phosphorylation of PDK1, independent of PTEN status. Dysregulation of AKT signaling pathway is known to drive drug resistance in various malignances with involving extensive crosstalk with other cell signaling networks. The efficacy of AKT targeted therapeutic strategies has been validated in preclinical and clinical trials [53].

Enzalutamide treatment has been found to activate the AKT signaling pathway through the stabilization of AKT phosphatase, thus promoting the development of ENZR [54]. Targeting AKT signaling pathway, which has been considered in primary PCa, maybe a promising approach to overcome androgen targeted therapy failure. Combination of AKT inhibitors, AZD5343, and enzalutamide markedly postponed the onset of ENZR by enhancing apoptosis and inducing cell cycle arrest [4]. Other AKT inhibitors are being studied in clinical trials, using liquid biopsies and genomic profiling to personalize cancer therapy [55]. To achieve clinical implication of AKT inhibitors, it is still necessary to nominate biomarkers to screening potential candidates and monitoring treatment effectiveness.

Axon guidance pathway is frequently altered, and likely be to a pathogenesis of PCa [18]. In both primary PCa and CRPC setting, a certain proportion of patients carry PLXNA1 amplification, which results in augment PLXNA1 mRNA level [16,23]. The accumulation of PLXNA1 leads to the recruitment of NRP1, which in turn catalyzes the phosphorylation of AKT in PCa cells. The analysis of transcriptomic data from PCa patients revealed the enrichment of the AKT signaling in both CRPC and primary PCa patients carrying PLXNA1 amplification. These findings underscore the potential clinical significance of AKT inhibitors within this subgroup.

This study elucidated the involvement of dysregulated PLXNA1 expression in ENZR development. Furthermore, we observed that perifosine efficiently inhibited the proliferation of ENZR cells, both independently and when combined with enzalutamide. Therefore, this innovative combination approach merits consideration for clinical trials aimed at overcoming ENZR in PCa. However, our study was mainly built with cell line models which is easily genetically manipulated and pharmacologically tested. The cell models only represent the clonal population of PCa and do not fully recapitulate tumor heterogeneity and individual diversity, both of which play a role in treatment resistance. Additionally, our ENZR cell models, even when used in xenograft experiments, were unable to fully encompass the complex interactions between PCa cells and mesenchymal or immune cells during ENZR

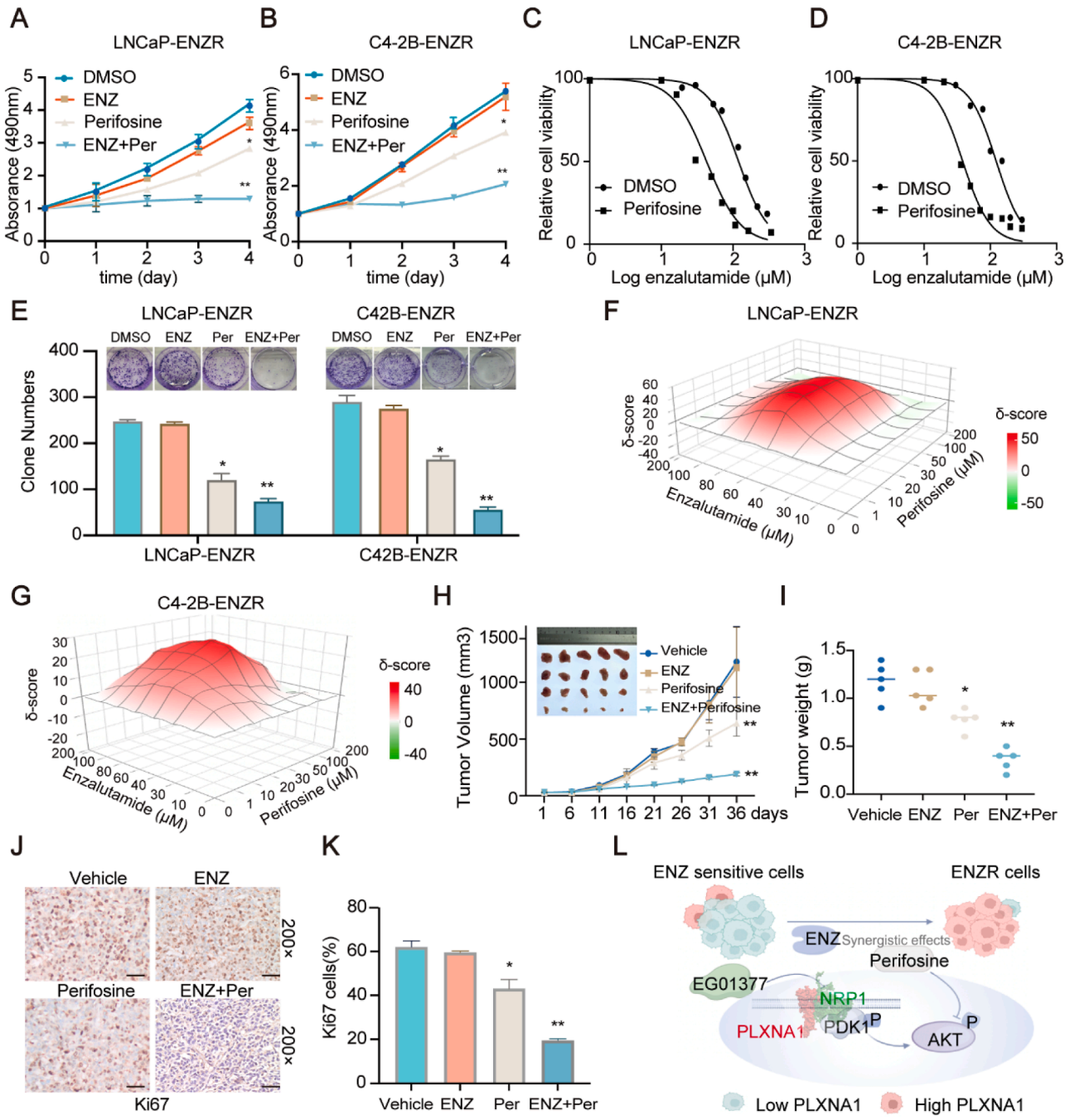

Fig. 6. Perifosine inhibits growth of enzalutamide resistant PCa.
(A-B) Cell viability was assessed by MTS assay. LNCaP-ENZR and C4-2B-ENZR cells were treated with DMSO, enzalutamide (20 μM), perifosine (10 μM) or in combination for 0-4 days. (C-D) Cell viability was measured in the indicated cell lines under enzalutamide treatment. LNCaP-ENZR and C4-2B-ENZR cells were seeded in 96-well plates, 24 h later, these cells were exposed to enzalutamide with −/+ perifosine (10 μM) for 3 days. Cell viability was measured by MTS assays. (E) Clonal assay of indicated cells with perifosine alone or in combination with enzalutamide. LNCaP-ENZR (left) and C4-2B-ENZR (right) cells were treated with DMSO, enzalutamide (20 μM), perifosine (10 μM) or in combination. Colonogenic assay was performed, and colony numbers were quantified. (F-G) The 3D-plots showing effect on cell growth and drug synergism of perifosine and/or enzalutamide at varied concentrations in LNCaP-ENZR and C4-2B-ENZR cells. (H-K) Mice bearing C4-2B-ENZR xenografts were treated with vehicle control, enzalutamide (10 mg kg^{-1} p.o.), perifosine (100 mg kg^{-1} p.o.), or their combination for 4 weeks (n = 5/group). Tumor volumes were measured 2 to 5 days. Tumors were collected, photographed and weighed (H-I) when mice were sacrificed. IHC staining of Ki67 on tumor slide from each group were shown (J-K). (L) A putative schematic diagram illustrating the role of PLXNA1 in contributing to ENZR. Data are represented as mean ± SD of three independent experiments. The Mann-Whitney U test was employed to compare differences among variables. *P<0.05, **P<0.01, ***P<0.001.

development. To translate our findings to clinical setting, further investigation with more sophisticated models, such as organoid, or patient derived xenograft (PDX) model is needed. Tissue engineering advancements now facilitate the creation of PDX from both primary and metastatic PCa lesions. These PDX models hold promise for the development of novel strategies in cancer precision medicine, bridging the gap between laboratory research and clinical applications [56].

In conclusion, our findings suggest that PLXNA1 may facilitate the progression of ENZR by recruiting NRP1 to activate AKT phosphorylation. Combining perifosine with enzalutamide may offer a more

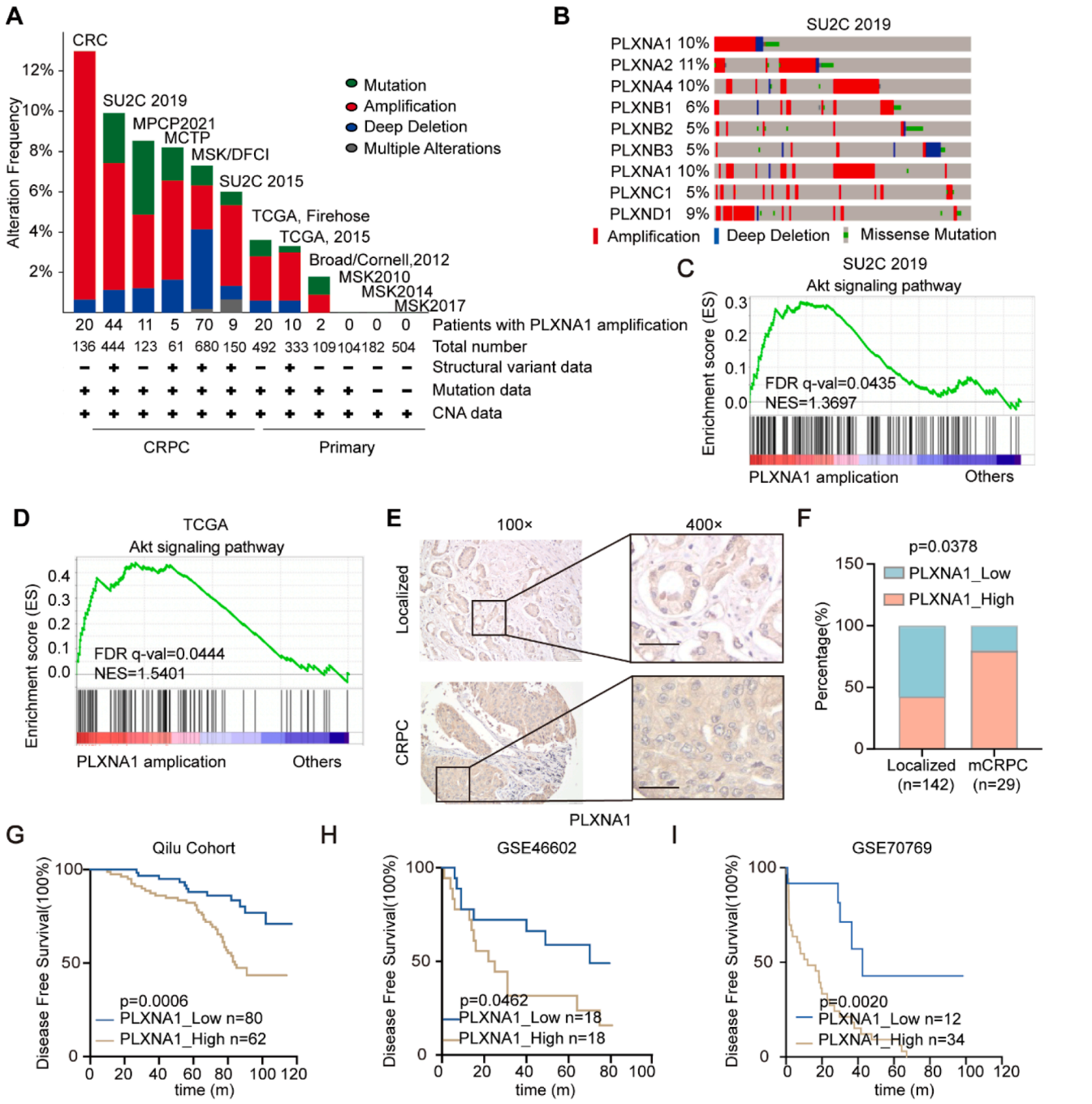

Fig. 7. PLXNA1 amplification correlates with AKT signaling pathway and PCa prognosis.
(A) Molecular profiles of PLXNA1 in primary PCa and CRPC according to cBiopartal for Cancer Genomics. (B) Copy-number variations (CNVs) of axon guidance pathway receptors in CRPC according to SU2C 2019 data (n=444). (C-D) Enrichment of AKT signaling pathway in CRPC and primary PCa patients harboring PLXNA1 amplification. SU2C 2019 data were used as CRPC cohort and TCGA data for primary PCa. (E-F) PLXNA1 expression assessed by IHC in localized and CRPC tissues in Qilu cohort. Representative IHC images (E) and quantitative results (F) were shown. Scale bar, 50 μm. (G-I) Kaplan–Meier survival analysis of PCa cases according to high and low PLXNA1 expression levels. PCa cases in Qilu cohort, GSE46602 (50 % cut-off) and GSE70769 (25 % cut-off) were stratified based on PLXNA1 expression levels and analyzed for disease-free survival. Survival analysis was conducted using the Kaplan-Meier method along with Log-rank tests. m, months.

effective approach to suppress the progression of ENZR. These results enhance our understanding of ENZR development and propose a promising strategy for intervention in its progression.

Ethics declarations

Ethics approval and consent to participate

Approval for this study was obtained from the Medical Research Ethics Committee of Qilu Hospital, Shandong University, in accordance with the principles of the Declaration of Helsinki (Document No ECSBMSSDU2021-1-61, date: February 29, 2020). All animal experiments were conducted in accordance with the Basel Declaration and approved by the Institutional Animal Care and Use Committee of Qilu Hospital, Shandong University (Document No ECSBMSSDU2021-1-61, date: February 29, 2020). Our animal experiments comply with regulations, ensuring that the size of solid tumors does not exceed 10 % of the animal's body weight. We confirm that the maximum tumor volume has

not been exceeded.

CRediT authorship contribution statement

Jing Hu: Writing – review & editing, Methodology. **Jing Zhang:** Project administration, Funding acquisition. **Bo Han:** Writing – review & editing, Methodology, Funding acquisition. **Ying Qu:** Methodology. **Qian Zhang:** Methodology. **Zeyuan Yu:** Investigation. **Lin Zhang:** Investigation. **Jingying Han:** Investigation. **Hui Liu:** Investigation. **Lin Gao:** Methodology. **Tingting Feng:** Investigation. **Baokai Dou:** Methodology. **Weiwen Chen:** Supervision. **Feifei Sun:** Writing – review & editing, Visualization, Investigation, Funding acquisition, Data curation.

Declaration of competing interest

The authors declare that they have no known competing financial interests or personal relationships that could have appeared to influence the work reported in this paper.

Acknowledgements

This work received support from the Natural Science Foundation of Shandong Province (ZR2022MH317, ZR2023QH046), the Joint Research Fund of Natural Science, Shandong Province (ZR2019LZL014), and the National Natural Science Foundation of China (Grant No 81972416, 82172818, 82303905).

Contributions

Bo Han, Jing Hu, Feifei Sun and Jing Zhang were involved in conceptualization, writing, review, and editing. Feifei Sun, Lin Zhang, Zeyuan Yu, Jingying Han, Hui Liu, Ying Qu, Baokai Dou, Tingting Feng, Lin Gao, and Qian Zhang planned the methodology, conducted the investigation, and contributed to the writing of the original draft. Bo Han, Feifei Sun, Weiwen Chen, and Jing Zhang supervised the project, managed the administration, and acquired funding. All authors reviewed manuscript drafts, provided edits, and approved the final manuscript.

Data availability

All data and material during the current study are available from the corresponding author on reasonable request.

Supplementary materials

Supplementary material associated with this article can be found, in the online version, at doi:10.1016/j.neo.2024.101047.

References

[1] R.L. Siegel, et al., Cancer statistics, 2022, CA Cancer J. Clin. 72 (1) (2022) 7–33.
[2] M. Kirby, C. Hirst, E.D. Crawford, Characterising the castration-resistant prostate cancer population: a systematic review, Int. J. Clin. Pract. 65 (11) (2011) 1180–1192.
[3] M.T. Schweizer, E.Y. Yu, Persistent androgen receptor addiction in castration-resistant prostate cancer, J. Hematol. Oncol. 8 (2015) 128.
[4] P. Toren, et al., Combination AZD5363 with enzalutamide significantly delays enzalutamide-resistant prostate cancer in preclinical models, Eur. Urol. 67 (6) (2015) 986–990.
[5] H.I. Scher, et al., Increased survival with enzalutamide in prostate cancer after chemotherapy, N. Engl. J. Med. 367 (13) (2012) 1187–1197.
[6] B.S. Taylor, et al., Integrative genomic profiling of human prostate cancer, Cancer Cell 18 (1) (2010) 11–22.
[7] X. Lu, et al., Quercetin reverses docetaxel resistance in prostate cancer via androgen receptor and PI3K/Akt signaling pathways, Int. J. Biol. Sci. 16 (7) (2020) 1121–1134.
[8] S.J. Crabb, et al., Overall survival update for patients with metastatic castration-resistant prostate cancer treated with capivasertib and docetaxel in the phase 2 ProCAID clinical trial, Eur. Urol. 82 (5) (2022) 512–515.
[9] M.P. Kolinsky, et al., A phase I dose-escalation study of enzalutamide in combination with the AKT inhibitor AZD5363 (capivasertib) in patients with metastatic castration-resistant prostate cancer, Ann. Oncol. 31 (5) (2020) 619–625.
[10] M.W. Muller, et al., Association of axon guidance factor semaphorin 3A with poor outcome in pancreatic cancer, Int. J. Cancer 121 (11) (2007) 2421–2433.
[11] G.C. Dworschak, et al., Biallelic and monoallelic variants in PLXNA1 are implicated in a novel neurodevelopmental disorder with variable cerebral and eye anomalies, Genet. Med. 23 (9) (2021) 1715–1725.
[12] S.A. O'Shea, et al., Neuropathological findings in a case of parkinsonism and developmental delay associated with a monoallelic variant in PLXNA1, Mov. Disord. 36 (11) (2021) 2681–2687.
[13] M.S. Jahan, et al., PlexinA1 deficiency in BALB/cAJ mice leads to excessive self-grooming and reduced prepulse inhibition, IBRo Rep. 9 (2020) 276–289.
[14] D. Yamada, et al., Plexin A1 signaling confers malignant phenotypes in lung cancer cells, Biochem. Biophys. Res. Commun. 480 (1) (2016) 75–80.
[15] A. Catalano, et al., The plexin-A1 receptor activates vascular endothelial growth factor-receptor 2 and nuclear factor-kappaB to mediate survival and anchorage-independent growth of malignant mesothelioma cells, Cancer Res. 69 (4) (2009) 1485–1493.
[16] W.W. Wang, et al., MicroRNA-134 prevents the progression of esophageal squamous cell carcinoma via the PLXNA1-mediated MAPK signalling pathway, EBioMedicine 46 (2019) 66–78.
[17] D.M.O. Higgins, et al., Semaphorin 3A mediated brain tumor stem cell proliferation and invasion in EGFRviii mutant gliomas, BMC. Cancer 20 (1) (2020) 1213.
[18] S. Ren, et al., Whole-genome and Transcriptome Sequencing of Prostate Cancer Identify New Genetic Alterations Driving Disease Progression, Eur. Urol. 73 (3) (2018) 322–339.
[19] Z. Zhang, et al., Inhibition of the Wnt/beta-catenin pathway overcomes resistance to enzalutamide in castration-resistant prostate cancer, Cancer Res. 78 (12) (2018) 3147–3162.
[20] F. Sun, et al., RUVBL1 promotes enzalutamide resistance of prostate tumors through the PLXNA1-CRAF-MAPK pathway, Oncogene 41 (23) (2022) 3239–3250.
[21] L. Gao, et al., KIF15-mediated stabilization of AR and AR-V7 contributes to enzalutamide resistance in prostate cancer, Cancer Res. 81 (4) (2021) 1026–1039.
[22] V.K. Arora, et al., Glucocorticoid receptor confers resistance to antiandrogens by bypassing androgen receptor blockade, Cell 155 (6) (2013) 1309–1322.
[23] M. Ghashghaei, et al., Identification of a radiosensitivity molecular signature induced by enzalutamide in hormone-sensitive and hormone-resistant prostate cancer cells, Sci. Rep. 9 (1) (2019) 8838.
[24] S. Kregel, et al., Acquired resistance to the second-generation androgen receptor antagonist enzalutamide in castration-resistant prostate cancer, Oncotarget. 7 (18) (2016) 26259–26274.
[25] J. Guerrero, et al., Enzalutamide, an androgen receptor signaling inhibitor, induces tumor regression in a mouse model of castration-resistant prostate cancer, Prostate 73 (12) (2013) 1291–1305.
[26] C. Liu, et al., Intracrine androgens and AKR1C3 activation confer resistance to enzalutamide in prostate cancer, Cancer Res. 75 (7) (2015) 1413–1422.
[27] U.R. Chandran, et al., Gene expression profiles of prostate cancer reveal involvement of multiple molecular pathways in the metastatic process, BMC. Cancer 7 (2007) 64.
[28] K.H. Tang, et al., CD133(+) liver tumor-initiating cells promote tumor angiogenesis, growth, and self-renewal through neurotensin/interleukin-8/CXCL1 signaling, Hepatology 55 (3) (2012) 807–820.
[29] M.M. Mortensen, et al., Expression profiling of prostate cancer tissue delineates genes associated with recurrence after prostatectomy, Sci. Rep. 5 (2015) 16018.
[30] S.T. Borno, et al., Genome-wide DNA methylation events in TMPRSS2-ERG fusion-negative prostate cancers implicate an EZH2-dependent mechanism with miR-26a hypermethylation, Cancer Discov. 2 (11) (2012) 1024–1035.
[31] J.Y. Dai, et al., DNA methylation and cis-regulation of gene expression by prostate cancer risk SNPs, PLoS. Genet. 16 (3) (2020) e1008667.
[32] H. Ross-Adams, et al., Integration of copy number and transcriptomics provides risk stratification in prostate cancer: A discovery and validation cohort study, EBioMedicine 2 (9) (2015) 1133–1144.
[33] A. Zhang, et al., LncRNA HOTAIR enhances the androgen-receptor-mediated transcriptional program and drives castration-resistant prostate cancer, Cell Rep. 13 (1) (2015) 209–221.
[34] Y. Zhao, et al., Activation of P-TEFb by androgen receptor-regulated enhancer RNAs in castration-resistant prostate cancer, Cell Rep. 15 (3) (2016) 599–610.
[35] A. Subramanian, et al., Gene set enrichment analysis: a knowledge-based approach for interpreting genome-wide expression profiles, Proc. Natl. Acad. Sci. U S A, 102 (43) (2005) 15545–15550.
[36] V.K. Mootha, et al., PGC-1alpha-responsive genes involved in oxidative phosphorylation are coordinately downregulated in human diabetes, Nat. Genet. 34 (3) (2003) 267–273.
[37] D.T. Miyamoto, et al., RNA-Seq of single prostate CTCs implicates noncanonical Wnt signaling in antiandrogen resistance, Science 349 (6254) (2015) 1351–1356.
[38] L. Telley, et al., Dual function of NRP1 in axon guidance and subcellular target recognition in cerebellum, Neuron 91 (6) (2016) 1276–1291.
[39] P. Zhang, et al., NRP1 promotes prostate cancer progression via modulating EGFR-dependent AKT pathway activation, Cell Death. Dis. 14 (2) (2023) 159.
[40] D.R. Alessi, et al., Characterization of a 3-phosphoinositide-dependent protein kinase which phosphorylates and activates protein kinase Balpha, Curr. Biol. 7 (4) (1997) 261–269.
[41] Y. Kong, et al., Structural basis for plexin activation and regulation, Neuron 91 (3) (2016) 548–560.

[42] A.A. van der Klaauw, et al., Human semaphorin 3 variants link melanocortin circuit development and energy balance, Cell 176 (4) (2019) 729–742, e18.
[43] C.A. Staton, et al., Expression of class 3 semaphorins and their receptors in human breast neoplasia, Histopathology 59 (2) (2011) 274–282.
[44] L. Yin, et al., MAOA promotes prostate cancer cell perineural invasion through SEMA3C/PlexinA2/NRP1-cMET signaling, Oncogene 40 (7) (2021) 1362–1374.
[45] Y. Lu, et al., Isoprenaline/beta2-AR activates Plexin-A1/VEGFR2 signals via VEGF secretion in gastric cancer cells to promote tumor angiogenesis, BMC. Cancer 17 (1) (2017) 875.
[46] N. Wang, et al., The Sema3A receptor Plexin-A1 suppresses supernumerary axons through Rap1 GTPases, Sci. Rep. 8 (1) (2018) 15647.
[47] G. Attard, E.S. Antonarakis, Prostate cancer: AR aberrations and resistance to abiraterone or enzalutamide, Nat. Rev. Urol. 13 (12) (2016) 697–698.
[48] S. Linder, et al., Drug-induced epigenomic plasticity reprograms circadian rhythm regulation to drive prostate cancer toward androgen independence, Cancer Discov. 12 (9) (2022) 2074–2097.
[49] P. Isaacsson Velho, et al., Wnt-pathway activating mutations are associated with resistance to first-line abiraterone and enzalutamide in castration-resistant prostate cancer, Eur. Urol. 77 (1) (2020) 14–21.
[50] Y. He, et al., Targeting signaling pathways in prostate cancer: mechanisms and clinical trials, Signal. Transduct. Target. Ther. 7 (1) (2022) 198.
[51] B.S. Carver, et al., Reciprocal feedback regulation of PI3K and androgen receptor signaling in PTEN-deficient prostate cancer, Cancer Cell 19 (5) (2011) 575–586.
[52] P. Xia, X.Y. Xu, PI3K/Akt/mTOR signaling pathway in cancer stem cells: from basic research to clinical application, Am. J. Cancer Res. 5 (5) (2015) 1602–1609.
[53] Y. Wang, et al., Mechanisms of enzalutamide resistance in castration-resistant prostate cancer and therapeutic strategies to overcome it, Br. J. Pharmacol. 178 (2) (2021) 239–261.
[54] H. Wenjing, et al., Exendin-4 enhances the sensitivity of prostate cancer to enzalutamide by targeting Akt activation, Prostate 80 (5) (2020) 367–375.
[55] H. Hua, et al., Targeting Akt in cancer for precision therapy, J. Hematol. Oncol. 14 (1) (2021) 128.
[56] M.G. Lawrence, et al., The future of patient-derived xenografts in prostate cancer research, Nat. Rev. Urol. 20 (6) (2023) 371–384.